ARTICLES

Repetitive shuttling of a motor protein on DNA

Sua Myong[1], Ivan Rasnik[1], Chirlmin Joo[1], Timothy M. Lohman[3] & Taekjip Ha[1,2]

Many helicases modulate recombination, an essential process that needs to be tightly controlled. Mutations in some human disease helicases cause increased recombination, genome instability and cancer. To elucidate the potential mode of action of these enzymes, here we developed a single-molecule fluorescence assay that can visualize DNA binding and translocation of *Escherichia coli* Rep, a superfamily 1 DNA helicase homologous to *Saccharomyces cerevisiae* Srs2. Individual Rep monomers were observed to move on single-stranded (ss)DNA in the 3′ to 5′ direction using ATP hydrolysis. Strikingly, on hitting a blockade, such as duplex DNA or streptavidin, the protein abruptly snapped back close to its initial position, followed by further cycles of translocation and snapback. This repetitive shuttling is likely to be caused by a blockade-induced protein conformational change that enhances DNA affinity for the protein's secondary DNA binding site, thereby resulting in a transient DNA loop. Repetitive shuttling was also observed on ssDNA bounded by a stalled replication fork and an Okazaki fragment analogue, and the presence of Rep delayed formation of a filament of recombination protein RecA on ssDNA. Thus, the binding of a single Rep monomer to a stalled replication fork can lead to repetitive shuttling along the single-stranded region, possibly keeping the DNA clear of toxic recombination intermediates.

The diverse activities of helicases, such as duplex nucleic acid unwinding[1], protein displacement[2,3], and branch migration[4], are powered by a common engine that translocates directionally on nucleic acids[5–7]. For example, yeast Srs2 helicase[8,9] and its bacterial homologues[10] disrupt recombination intermediates formed around ssDNA, probably driven by DNA translocation. We investigated the translocation mechanisms of *E. coli* Rep, an Srs2 homologue that functions in replication restart[11,12] and replication of certain phages[13].

We engineered single-cysteine mutants of Rep that retain activity *in vivo* and with and without dye labels *in vitro*[14]. Although a Rep monomer cannot unwind DNA *in vitro*[15–17], it can translocate on ssDNA in the 3′ to 5′ direction using ATP hydrolysis[17]. The single cysteine was labelled with a donor fluorophore (Cy3) with 90% efficiency[14] and the movement of a donor-labelled Rep on an acceptor (Cy5)-labelled DNA was detected by single-molecule fluorescence resonance energy transfer (FRET)[18–20]. To optimize the FRET signal, the donor was attached to the position 333 ('leading-edge'[21]) for an acceptor at the 5′ end of ssDNA, or to the position 43 ('trailing-edge'[21]) for an acceptor at the 3′ end. Double-stranded (ds)DNA (18 base pairs, bp) with a 3′ $(dT)_n$ tail ($n = 40$, 60 or 80) and a Cy5 attached to the junction was tethered at the duplex end to a polymer-coated quartz slide via biotin–streptavidin, and single-molecule data were obtained in the presence of 300 pM of Rep and 1 mM ATP in solution using dual-view wide-field total-internal-reflection fluorescence microscopy[14,16,22] with 15-ms time resolution (Fig. 1a and Supplementary Fig. S1). Direct excitation of the acceptor at the donor-excitation wavelength of 532 nm is insignificant and the polymer coating eliminates nonspecific surface binding of proteins[14,16,23], so single-molecule fluorescence signals are observed only when the protein binds the DNA.

Blockade-induced repetitive shuttling of a Rep monomer on DNA

When a Rep monomer (Cy3 labelled at position 333) binds the partial duplex DNA with a $(dT)_{80}$ tail, the donor fluorescence signal rises abruptly, combined with a weak acceptor signal (Fig. 1b). This is followed by a gradual decrease in donor signal and a concomitant gradual increase in acceptor signal (and corresponding FRET increase, Fig. 1d), consistent with ssDNA translocation in the 3′ to 5′ direction towards the junction. Since Rep cannot unwind duplex DNA as a monomer *in vitro*[15,16], the junction presents itself as a blockade at which the protein is expected to stop and dissociate. Instead of the anticipated dissociation, however, we observed an instantaneous (within 15 ms) FRET decrease to near the initial value (Fig. 1b and d) which is followed by further cycles of a gradual FRET increase and an abrupt FRET decrease. This sawtooth-shaped cycle was repeated several times until it was finally terminated by protein dissociation or photobleaching. We interpret the sawtooth pattern as reflecting repeated cycles of ssDNA translocation followed by the protein snapback to near its initial binding region (see below) and will call it 'repetitive shuttling' henceforth. Repetitive shuttling was observed over a wide range of solution conditions (15–100 mM NaCl, 2.1–10 mM $MgCl_2$, 22–37 °C) and also with DNA containing ssDNA tails of mixed sequences (Fig. 1c, Supplementary Figs S2, S3 and S5). Typically, more than 80% of binding events resulted in repetitive shuttling (Supplementary Fig. S2).

Several lines of evidence strongly suggest that the sawtooth pattern is caused by a single Rep monomer rather than successive binding of different monomers. (1) Because the labelling efficiency is about 90%, a single monomer can be discerned by the well-defined fluorescence intensity of a single donor[14]. (2) Sawtooth patterns are observed as well-isolated bursts (Fig. 1b and c). (3) When a flow of buffer devoid of protein was applied during data acquisition to remove free proteins in solution, the sawtooth patterns persisted.

Figures 1d–f show histograms of the time between two successive snapbacks, Δt. The peak of the histogram shifts to longer times as the tail length increases (0.62, 1.0 and 1.23 s for 40, 60 and 80 nucleotide (nt) tails, respectively), suggesting that the gradual FRET increase corresponds to ssDNA translocation. Single-molecule FRET time

[1]Physics Department, University of Illinois, Urbana-Champaign, and [2]Howard Hughes Medical Institute, Urbana, Illinois 61801, USA. [3]Department of Biochemistry and Molecular Biophysics, Washington University School of Medicine, St Louis, Missouri 63110, USA.

traces show that the protein spends longer times in the low FRET phase for longer ssDNA tails, consistent with this interpretation (Figs 1d–f). A sawtooth pattern with a 2.7 s period was observed using a similar DNA with a 182-nt 3′ tail of mixed sequence (Supplementary Fig. S3), further supporting our interpretation. The period of the sawtooth pattern increases at low ATP concentrations or when 10–20 μM ATPγS is added to a high concentration of ATP (Supplementary Fig. S4), strongly implicating ssDNA translocation powered by ATP hydrolysis. The closest distance between the two dyes is about 4–5 nm (FRET efficiency ~0.75 and R_0 of 5–6.3 nm; refs 14, 23), consistent with the structure of another superfamily 1 DNA helicase, PcrA of *Bacillus stearothermophilus*, bound to a partial duplex junction[24]. The remarkable regularity of the sawtooth pattern and narrowly peaked Δt histograms suggest that the site for the re-initiation of translocation is not random and is likely to be localized near the 3′ end. The linear relation between the period and the tail length further suggests that snapback redirects the protein primarily to a region near the 3′ end. The ssDNA translocation rates estimated from the single-molecule experiments agree with those obtained from ensemble studies with unmodified Rep when both are performed under similar conditions (Supplementary Fig. S5).

We observed similar sawtooth patterns (average period = 1.2 s) when a ssDNA, $(dT)_{50}$, is terminated at the 5′ end by a biotin bound to a streptavidin (Fig. 1g and h). Because the acceptor is near the 3′ end, we observe a gradual FRET decrease during translocation followed by an abrupt FRET increase. In contrast, only single translocation events followed by dissociation were observed when the 3′ end is attached to a streptavidin and the 5′ end is free (Fig. 1i and j). These observations suggest that the encounter of a physical blockade such as duplex DNA junction or streptavidin may trigger a snapback.

In contrast to the previously observed backward movements of RecBCD[25] and UvrD[26], repetitive shuttling of Rep is (1) deterministic, that is, the forward and backward movements are repeated in regular intervals and are reliably triggered by a blockade, (2) highly asymmetric so that the backward movement occurs too fast to be resolved, and (3) observed without applied force.

Physical mechanisms of repetitive shuttling

Rep binds to ssDNA with a rate constant ~20 times slower than the diffusion-limited value[15], so a Rep that dissociates completely from DNA is much more likely to diffuse away than to rebind to the same DNA. Therefore, repetitive shuttling is unlikely to be due to complete dissociation and rebinding of Rep. To remain bound to the DNA during snapback, the protein either has to slide all the way towards the 3′ end in less than 15 ms, or has to make simultaneous contacts with the junction and the 3′ end. We favour the latter mechanism, on the basis of the following studies of DNA conformations during translocation (Fig. 2a). In the presence of unlabelled Rep and ATP, a DNA with a 3′ $(dT)_{40}$ tail labelled at the near extremities with a donor and an acceptor showed mostly low FRET values (~0.4) but with brief, regular spikes to high FRET efficiency (~0.7; spikes had average duration 0.17 s) (Fig. 2b). No such spikes were observed from DNA alone. The average period of this pattern is 0.7 s, very similar to the period of the sawtooth pattern observed with labelled Rep translocating along a 40-nt tail. We therefore interpret the high FRET spike as reflecting the simultaneous binding of Rep to both the junction and the 3′ end of the ssDNA, resulting in the transient formation of a DNA loop. This mechanism requires at least two distinct DNA binding sites on the Rep monomer, the primary binding site as observed in crystal structures[24,27] and the secondary binding site for the 3′ end. We suggest that a blockade encounter induces Rep conformational changes that increase the DNA affinity of the secondary binding site. The loop formation can follow immediately because ssDNA is highly flexible and its conformational fluctuations are much faster than our time resolution[28].

We next investigated whether Rep undergoes conformational changes coupled with repetitive shuttling. Rep is structurally homologous to another superfamily 1 helicase PcrA, and is composed of

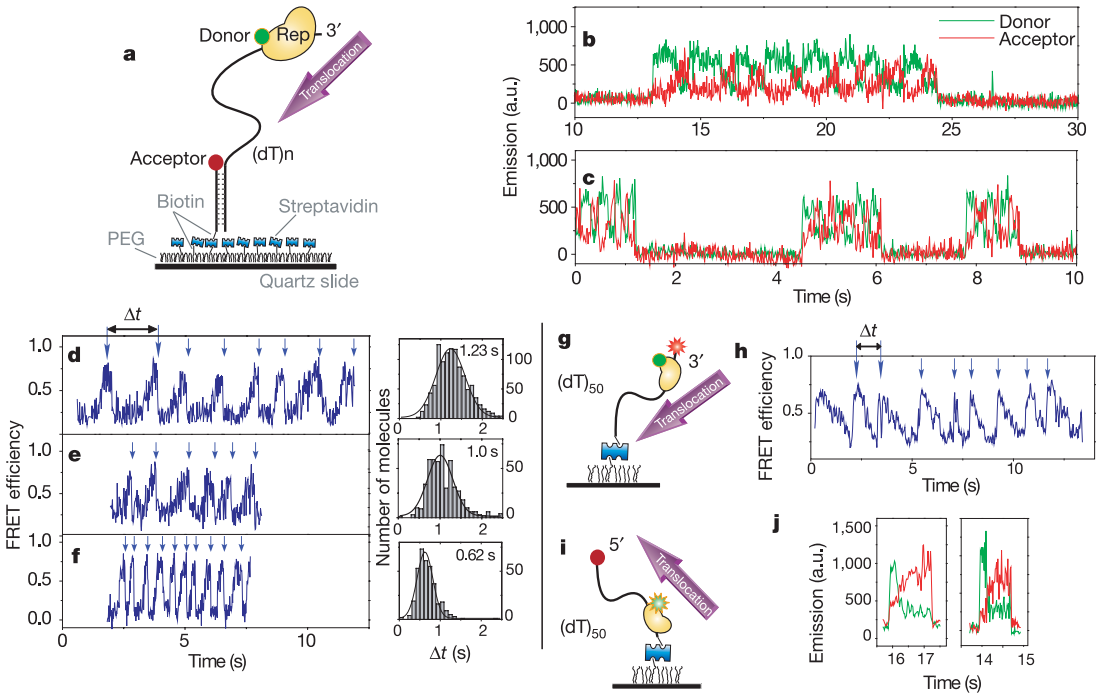

Figure 1 | Blockade-induced repetitive shuttling. **a**, Donor-labelled Rep binds to a 3′ ssDNA tail and translocates towards the acceptor. **b**, **c**, Fluorescence intensity traces for a 3′ $(dT)_{80}$ tail at 22 °C (**b**) and 37 °C (**c**). **d**–**f**, FRET traces for 3′ tails of 80, 60 and 40 dTs. Histograms of Δt between snapbacks (arrows) are shown with gaussian fits (solid lines). **g**, Donor-labelled Rep moves away from the acceptor towards streptavidin. **h**, Repeated cycles of gradual decrease and abrupt increase of FRET. **i**, Donor-labelled Rep moves towards the acceptor and away from streptavidin. **j**, Only gradual FRET increase was observed. a.u., arbitrary units.

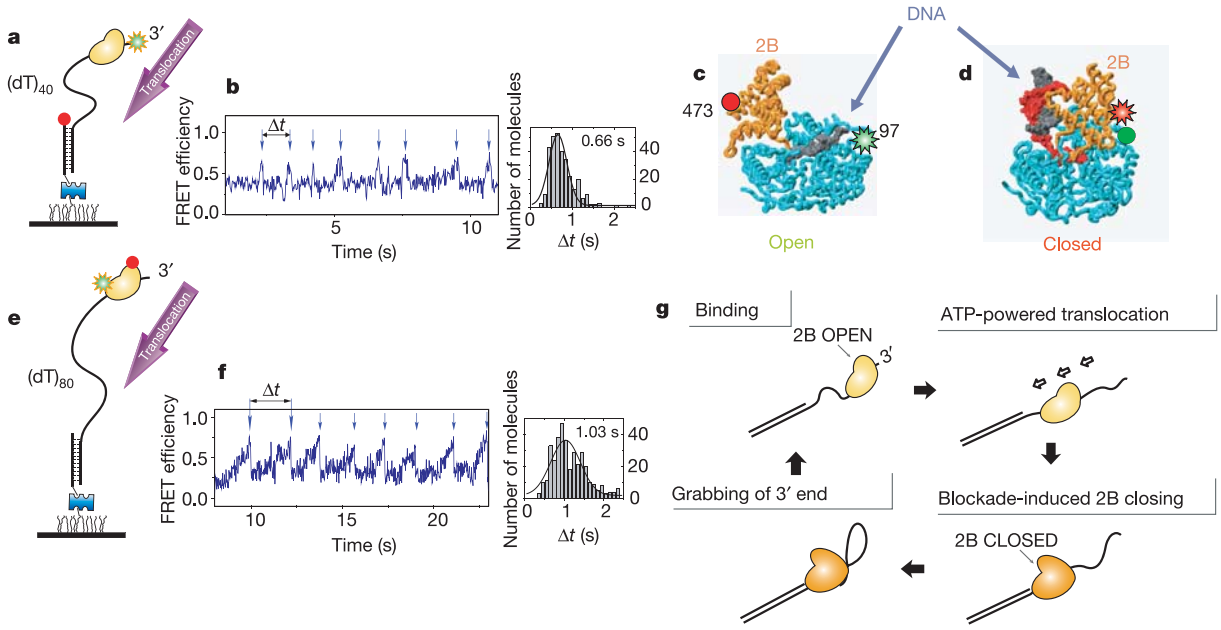

Figure 2 | Physical mechanism of repetitive shuttling. **a**, Unlabelled Rep moves on a dual-labelled $(dT)_{40}$ tail. **b**, FRET trace shows brief spikes to high FRET (arrows); the Δt histogram shows a gaussian fit (solid line) **c**, Crystal structure of Rep (2B in orange and the rest in blue) bound to ssDNA (grey). Red and green symbols denote cysteines at residues 473 and 97. **d**, PcrA structure bound to a partial duplex DNA. Residues equivalent to residues 473 and 97 of Rep are marked with red and green symbols. **e**, Dual-labelled Rep moves on a $(dT)_{80}$ tail. **f**, Repeated cycles of gradual FRET increase and abrupt FRET decrease. The Δt histogram with a gaussian fit (solid line) is shown. **g**, Rep undergoes conformational changes upon blockade approach, transfer to 3′ end via a DNA loop, and restart of translocation.

four subdomains (1A, 2A, 1B and 2B)[24,27]. The 2B subdomain of Rep is dispensable for unwinding[29] and ssDNA translocation[17]. Rep was crystallized in two forms, open (Fig. 2c) and closed, which differ in the 2B subdomain orientation[27]. A PcrA bound to a 3′-tailed dsDNA was crystallized in the closed form (Fig. 2d)[24] and Rep bound to a 3′-tailed dsDNA in solution favours the closed form[14]. To test whether the 2B subdomain closes as Rep approaches the junction, we engineered a double-cysteine mutant of Rep (positions 97 and 473 on the 1B and 2B subdomains, respectively) and labelled it stochastically with Cy3 and Cy5 so that 2B closing would result in a FRET increase (Fig. 2c and d). Single-molecule measurements could identify this mutant labelled with one donor and one acceptor[30] as it moves on unlabelled DNA with a 3′ $(dT)_{80}$ tail (Fig. 2e). A representative time trace in Fig. 2f shows several cycles of gradual FRET increase and an abrupt FRET decrease. The shortest distance between the donor and acceptor fluorophores on Rep is estimated to

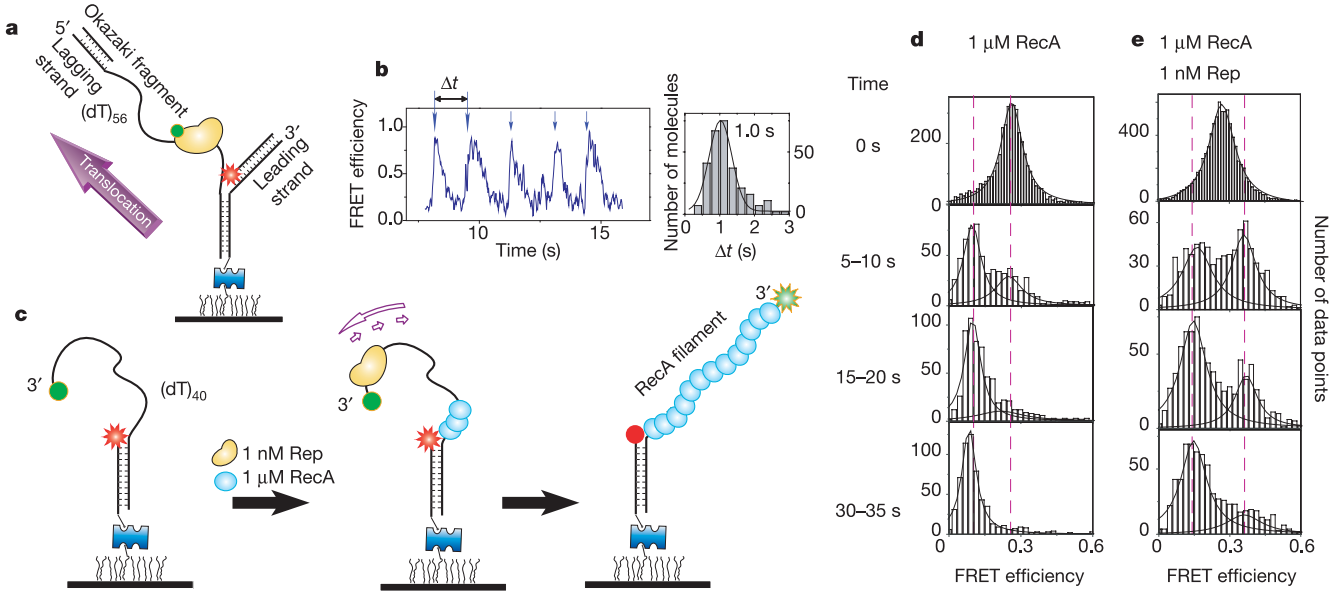

Figure 3 | Potential roles of repetitive shuttling. **a**, Donor-labelled Rep moves on $(dT)_{56}$ between a replication fork and an Okazaki fragment analogue. **b**, FRET trace shows cycles of gradual decrease/abrupt increase. The Δt histogram with a gaussian fit (solid line) is shown. **c**, FRET detection of RecA filament formation on $(dT)_{40}$, which may be hindered by Rep. **d**, Time-dependent single-molecule FRET histograms of the DNA shown in **c** after adding RecA and ATP. Dashed lines denote the FRET values for the DNA only and the RecA filament. Also shown are the lorenzian fits. **e**, Same as in **d**, except for the inclusion of 1 nM Rep. The shift to higher FRET is probably due to Rep activity.

be 4–5 nm (FRET value ~0.75), in agreement with the closed form of the Rep structure (3-nm C_α distance plus dye linkers). Similar cycles of FRET changes were observed when the doubly labelled Rep mutant was moving on a $(dT)_{60}$ attached to a streptavidin via 5′-biotin (Supplementary Fig. S6). Thus, the 2B subdomain closes gradually as the protein approaches a blockade, and its complete closing may correlate with the affinity enhancement of the secondary binding site towards the 3′ end of the ssDNA, followed by the snapback and the restart of translocation (Fig. 2g and Supplementary Fig. S1). Single-molecule measurements with various ATP analogues suggest that the 2B subdomain opens and closes during each ATP hydrolysis cycle (our unpublished observations). Although the gradual FRET change observed here is surprising, it may reflect a rapid equilibration between the two conformations of the 2B domain whose midpoint shifts as the blockade is approached.

Potential roles of repetitive shuttling in replication restart

Next, we designed a DNA substrate that is relevant to Rep's function in replication restart (Fig. 3a)[11,12]. Rep binds with high affinity to a three-way junction with a 5′ overhang[12] that resembles a stalled replication fork with an incompletely synthesized lagging strand, suggesting that Rep may recognize a fork ready to be restarted. However, the role of Rep as a helicase is not clear in this context because its 3′–5′ translocation/unwinding activity would result in translocation towards the Okazaki fragment rather than unwinding the duplexes at the fork. The inability to unwind DNA (the Okazaki fragment) as a monomer, the high affinity for the fork structure, and the ability to snap back quickly may combine to allow a Rep monomer to shuttle back and forth multiple times on the ssDNA region before dissociation. Indeed, we observed the sawtooth pattern from such a structure with a ssDNA gap, $(dT)_{56}$, and an Okazaki fragment analogue (16 bp) (Fig. 3a and b). The time trace in Fig. 3b shows clear evidence of repetitive shuttling (period 1.0 s). This also shows that a free 3′ end is not the only DNA structure on which a snapback can be observed. Repetitive shuttling was also observed when the ssDNA gap was 56 nt of mixed sequence (Supplementary Fig. S7).

What might be the biological role of repetitive shuttling of Rep? Rep functions in the restart of stalled replication forks[11,12] and in the replication of certain phages[31], but the *in vivo* functional form (monomer, dimer, and so on) of this low-copy-number[32] protein is not known. Two other superfamily 1 helicases, yeast Srs2 (refs 8, 9) and *E. coli* UvrD[10], can displace Rad51 and RecA presynaptic filaments from ssDNA, respectively. Deletion of both Rep and UvrD is lethal in *E. coli*, and it was suggested that Rep prevents the formation of potentially toxic RecA filaments and that UvrD destroys the filament in the absence of Rep[10]. Such a preventative role of Rep is suggested by Rep's ability to interfere with RecA filament formation (Fig. 3d and e). Filament formation by RecA (at [RecA] = 1 μM) on $(dT)_{40}$ was monitored by FRET (Fig. 3c) and was observed to be delayed substantially even at Rep concentrations as low as 1 nM. *E. coli* remains viable even with the deletion of both Rep and UvrD if RecFOR machinery is defective[33]. RecFOR removes SSB from stalled replication forks and loads RecA[34], so the lethality of the double deletion of Rep and UvrD may indeed arise from uncontrolled recombination via the RecA filaments. On the basis of the present results, we propose that repetitive shuttling of Rep may be an effective means of keeping the ssDNA clear of unwanted proteins. Such a mode of action does not require the canonical helicase function of duplex unwinding, and therefore could be carried out by a Rep monomer. Whether a Rep monomer can indeed perform these functions *in vivo* is yet to be determined.

METHODS

Proteins were purified and labelled as described[14]. A quartz slide was coated with poly-ethylene glycol (PEG) and streptavidin as described[14,16,23]. After immobilizing biotinylated DNA (300 pM), images were obtained in the presence of 300 pM Rep in solution in a wide-field total-internal-reflection fluorescence microscope[14,16,23] with 15-ms time resolution using an electron multiplying charge-coupled device (CCD) camera (iXon DV 887-BI, Andor Technology) and a homemade C++ program written by S. A. McKinney (available on request). The Rep concentration used is much lower than the ~300 nM needed for efficient dimer formation and DNA unwinding *in vitro*[15]. All measurements were performed at 22 °C with the following buffer composition unless mentioned otherwise: 10 mM Tris-HCl, pH 7.6, 1 mM ATP, 12 mM $MgCl_2$, 15 mM NaCl, 10% glycerol (v/v), and an oxygen scavenger system[14] to slow photobleaching. Snapback events were visually identified and their timings were recorded using a MATLAB program (available on request). Single-molecule FRET histograms for RecA experiments were obtained by averaging over 1 s. RecA concentration used is within the range expected *in vivo*. FRET values were calculated as the ratio between the acceptor intensity and the total intensity. DNA sequences, modifications and annealing procedures are described in the Supplementary Information.

Received 15 May; accepted 21 July 2005.

1. Lohman, T. M. & Bjornson, K. P. Mechanisms of helicase-catalyzed DNA unwinding. *Annu. Rev. Biochem.* **65,** 169–214 (1996).
2. Byrd, A. K. & Raney, K. D. Protein displacement by an assembly of helicase molecules aligned along single-stranded DNA. *Nature Struct. Mol. Biol.* **11,** 531–538 (2004).
3. Fairman, M. E. *et al.* Protein displacement by DExH/D "RNA helicases" without duplex unwinding. *Science* **304,** 730–734 (2004).
4. Kaplan, D. L. & O'Donnell, M. DnaB drives DNA branch migration and dislodges proteins while encircling two DNA strands. *Mol. Cell* **10,** 647–657 (2002).
5. Lee, M. S. & Marians, K. J. Differential ATP requirements distinguish the DNA translocation and DNA unwinding activities of the *Escherichia coli* PRI A protein. *J. Biol. Chem.* **265,** 17078–17083 (1990).
6. Kawaoka, J., Jankowsky, E. & Pyle, A. M. Backbone tracking by the SF2 helicase NPH-II. *Nature Struct. Mol. Biol.* **11,** 526–530 (2004).
7. von Hippel, P. H. Helicases become mechanistically simpler and functionally more complex. *Nature Struct. Mol. Biol.* **11,** 494–496 (2004).
8. Krejci, L. *et al.* DNA helicase Srs2 disrupts the Rad51 presynaptic filament. *Nature* **423,** 305–309 (2003).
9. Veaute, X. *et al.* The Srs2 helicase prevents recombination by disrupting Rad51 nucleoprotein filaments. *Nature* **423,** 309–312 (2003).
10. Veaute, X. *et al.* UvrD helicase, unlike Rep helicase, dismantles RecA nucleoprotein filaments in *Escherichia coli*. *EMBO J.* **24,** 180–189 (2005).
11. Sandler, S. J. Multiple genetic pathways for restarting DNA replication forks in *Escherichia coli* K-12. *Genetics* **155,** 487–497 (2000).
12. Marians, K. J. Mechanisms of replication fork restart in *Escherichia coli*. *Phil. Trans. R. Soc. Lond. B* **359,** 71–77 (2004).
13. Scott, J. F., Eisenberg, S., Bertsch, L. L. & Kornberg, A. A mechanism of duplex DNA replication revealed by enzymatic studies of phage φX174: catalytic strand separation in advance of replication. *Proc. Natl Acad. Sci. USA* **74,** 193–197 (1977).
14. Rasnik, I., Myong, S., Cheng, W., Lohman, T. M. & Ha, T. DNA-binding orientation and domain conformation of the *E. coli* Rep helicase monomer bound to a partial duplex junction: Single-molecule studies of fluorescently labelled enzymes. *J. Mol. Biol.* **336,** 395–408 (2004).
15. Cheng, W., Hsieh, J., Brendza, K. M. & Lohman, T. M. *E. coli* Rep oligomers are required to initiate DNA unwinding *in vitro*. *J. Mol. Biol.* **310,** 327–350 (2001).
16. Ha, T. *et al.* Initiation and reinitiation of DNA unwinding by the *Escherichia coli* Rep helicase. *Nature* **419,** 638–641 (2002).
17. Brendza, K. M. *et al.* Auto-inhibition of *E. coli* Rep monomer helicase activity by its 2B sub-domain. *Proc. Natl Acad. Sci. USA* **102,** 10081 (2005).
18. Ha, T. *et al.* Probing the interaction between two single molecules—fluorescence resonance energy transfer between a single donor and a single acceptor. *Proc. Natl Acad. Sci. USA* **93,** 6264–6268 (1996).
19. Weiss, S. Fluorescence spectroscopy of single biomolecules. *Science* **283,** 1676–1683 (1999).
20. Ha, T. Single molecule fluorescence resonance energy transfer. *Methods* **25,** 78–86 (2001).
21. Mukhopadhyay, J. *et al.* Translocation of σ^{70} with RNA polymerase during transcription: fluorescence resonance energy transfer assay for movement relative to DNA. *Cell* **106,** 453–463 (2001).
22. Zhuang, X. W. *et al.* A single-molecule study of RNA catalysis and folding. *Science* **288,** 2048–2051 (2000).
23. Blanchard, S. C., Kim, H. D., Gonzalez, R. L. Jr, Puglisi, J. D. & Chu, S. tRNA dynamics on the ribosome during translation. *Proc. Natl Acad. Sci. USA* **101,** 12893–12898 (2004).
24. Velankar, S. S., Soultanas, P., Dillingham, M. S., Subramanya, H. S. & Wigley, D. B. Crystal structures of complexes of PcrA DNA helicase with a DNA substrate indicate an inchworm mechanism. *Cell* **97,** 75–84 (1999).
25. Perkins, T. T., Li, H. W., Dalal, R. V., Gelles, J. & Block, S. M. Forward and reverse motion of single RecBCD molecules on DNA. *Biophys. J.* **86,** 1640–1648 (2004).

26. Dessinges, M. N., Lionnet, T., Xi, X. G., Bensimon, D. & Croquette, V. Single-molecule assay reveals strand switching and enhanced processivity of UvrD. *Proc. Natl Acad. Sci. USA* **101,** 6439–6444 (2004).
27. Korolev, S., Hsieh, J., Gauss, G. H., Lohman, T. M. & Waksman, G. Major domain swiveling revealed by the crystal structures of complexes of *E. coli* Rep helicase bound to single-stranded DNA and ATP. *Cell* **90,** 635–647 (1997).
28. Murphy, M. C., Rasnik, I., Cheng, W., Lohman, T. M. & Ha, T. Probing single stranded DNA conformational flexibility using fluorescence spectroscopy. *Biophys. J.* **86,** 2530–2537 (2004).
29. Cheng, W. *et al.* The 2B domain of the *Escherichia coli* Rep protein is not required for DNA helicase activity. *Proc. Natl Acad. Sci. USA* **99,** 16006–16011 (2002).
30. Margittai, M. *et al.* Single-molecule fluorescence resonance energy transfer reveals a dynamic equilibrium between closed and open conformations of syntaxin 1. *Proc. Natl Acad. Sci. USA* **100,** 15516–15521 (2003).
31. Denhardt, D. T., Dressler, D. H. & Hathaway, A. The abortive replication of ϕX174 DNA in a recombination deficient mutant of *Escherichia coli*. *Proc. Natl Acad. Sci. USA* **57,** 813–820 (1967).
32. Scott, J. F. & Kornberg, A. Purification of the rep protein of *Escherichia coli*. An ATPase which separates duplex DNA strands in advance of replication. *J. Biol. Chem.* **253,** 3292–3297 (1978).
33. Petit, M. A. & Ehrlich, D. Essential bacterial helicases that counteract the toxicity of recombination proteins. *EMBO J.* **21,** 3137–3147 (2002).
34. Morimatsu, K. & Kowalczykowski, S. C. RecFOR proteins load RecA protein onto gapped DNA to accelerate DNA strand exchange: a universal step of recombinational repair. *Mol. Cell* **11,** 1337–1347 (2003).

Supplementary Information is linked to the online version of the paper at www.nature.com/nature.

Acknowledgements We thank S. A. McKinney for writing the data acquisition program and the National Institute of Health for grants (to T.H. and T.M.L.).

Author Information Reprints and permissions information is available at npg.nature.com/reprintsandpermissions. The authors declare no competing financial interests. Correspondence and requests for materials should be addressed to T.H. (tjha@uiuc.edu).